energies

MDPI

Article

Concept Assessment for an Application of a Crossflow Turbine Module for an In-Stream Hydropower System

Georgi Todorov [1], Konstantin Kamberov [1,*], Tsvetozar Ivanov [1] and Radoslav Miltchev [2]

[1] Department of Production Technology and Systems, Faculty of Industrial Technology, Technical University of Sofia, 1000 Sofia, Bulgaria; gdt@tu-sofia.bg (G.T.); ts.ivanov@tu-sofia.bg (T.I.)
[2] Department of Theory of Mechanisms and Machines, Faculty of Industrial Technology, Technical University of Sofia, 1000 Sofia, Bulgaria; rmiltchev@tu-sofia.bg
* Correspondence: kkamberov@tu-sofia.bg

Abstract

The study presents a concept assessment of a crossflow turbine with vertical-axis application in a "zero-head" system for rivers with high discharge. The evaluation of system output parameters, such as generated power and efficiency, is performed through numerical simulations over a virtual prototype. The approach used is validated in previous studies through a physical prototype of the downscaled system. The focus is on the virtual prototyping results for a single module of two Bánki–Michell/Ossberger turbines across a range of rotational speeds to assess system robustness. An overall efficiency of about 60% is calculated, indicating opportunities for design improvement. The obtained results relate to a complete channel system with five site stations, each with four modules. The study also includes a preliminary financial assessment of parameters, such as the investment period and the overall financial efficiency of such a solution. The main result of the study is an evaluated concept, with certain directions for further improvement in the next stage of detailed design development, using the validated simulation model.

Keywords: crossflow turbine; in-stream hydropower; virtual prototyping; numerical methods; CFD analysis

1. Introduction

The growing Earth population has certain demands, especially towards the quality of living. The world population reached 8 billion in November 2022 [1], and it has its needs for food and water, energy, housing/shelter, healthcare, and education [2]. One of these components—the energy—is obtained mainly using primary energy resources—renewable or non-renewable. Renewable energy harvesting is in the focus of actual research studies, aiming to develop the so-called green energy technologies [3]. The process of "decarbonization" aims to reduce the use of fossil fuels (which account for around 80% of global consumption) to mitigate climate change [4]. The development of green technologies is at the core of this decarbonization, referring to the use of the next generation of energy sources: solar, wind, hydro, geothermal, and bio. Solar energy has significant potential due to its permanent availability and the ability to generate megawatts of energy. Advances in solar energy harvesters (using the electromagnetic portion of solar energy rather than optical [5]) have reached 80% efficiency, making solar-based technology a popular solution [4]. A renewable source with low operating costs, wind energy is another key solution for reaching a green energy economy [6]. Wind-powered generators have always been a focus

Check for updates

Academic Editors: Helena M. Ramos and Lars Johanning

Received: 16 December 2025
Revised: 13 January 2026
Accepted: 21 January 2026
Published: 23 January 2026

Copyright: © 2026 by the authors. Licensee MDPI, Basel, Switzerland. This article is an open access article distributed under the terms and conditions of the Creative Commons Attribution (CC BY) license.

of modern power system development. This technology is influenced by the development of various electronic devices as control systems and by larger-capacity, cheaper turbines [7]. Another direction of improvement is the use of smart materials, enabling the production of larger and stronger wind turbines with enhanced performance [8–11].

Hydroenergy is a resource for the oldest large-scale power generation systems, including electrical power, and one of the world's largest and cheapest sources of renewable energy. It also accounts for almost a fifth of global electricity generation (18%, cited in [12]), and more than half of global renewable electricity generation [13]. This type of energy is also referred to as the most secure, efficient, and reliable, due to the extensive experience gained from its use over more than a hundred years [14]. This long period of development has resulted in many different technical solutions that can be grouped into two approaches—hydrostatic and hydrokinetic methods [15,16]. Hydrostatic power generation systems are widely used and can also act as "batteries," which are very efficient for balancing the electrical grid (pumped storage hydropower systems) [17,18]. Hydrostatic systems are experiencing rapid growth, especially in landscapes with denivelation (mountains, hills, etc.) [19].

Besides the intense ongoing development of hydrostatic systems, hydrokinetic systems are also of great interest. This type of energy harvester, also called "zero-head" hydropower systems, extracts the kinetic energy of flowing water, as with wind turbines, rather than the potential energy of water transport, which usually requires a head (hydrostatic). "Zero-head" systems have certain advantages over hydrostatic systems. They are relatively simple, require less construction work, and have minimal environmental impacts compared to dams [20]. Usually, their lower capacity is shown as a great disadvantage. The so-called "Betz limit" refers to the maximum efficiency of an instream hydrokinetic turbine of 59.3%, but certain studies report much higher values of about 80% [21–23], for systems with very low head. Recent research activities indicate a relative "revival" of this type of hydropower system [24–29].

Generally, by their application site, the hydrokinetic systems can be divided into tidal (or wave, as in oceans and seas) and river (or current) installations [30,31]. River systems could be classified by their design, such as turbines and water wheels. The hydrokinetic turbines are axial (or horizontal, with straight or inclined axis), radial (Darrieus, Gorlov, Savonius, and Bánki–Michell/Ossberger), and axial–radial [32–34]. This type of "zero-head" installation using turbines has been the subject of many recent studies and is promising [35,36]. A big part of these and other studies are performed using virtual prototyping simulations [13,35–40]. These studies also refer to Bánki–Michell/Ossberger (BMO) type of turbines, but mainly to installations with a horizontal axis [13,38–40]. Most of these previous studies on BMO cross-flow turbines applications are related to their numerical assessment and design through virtual prototyping [13,30,34,35,39,40]. The validation of the numerical results is specifically examined in [39], and a downsized, scaled, model is used for validation in [40]. The results of these studies give a sufficient basis for further study development, using this approach.

Virtual prototyping has become a common stage of the product design development process. This approach is used to assess the product performance at an early stage of its development, reducing time and cost [41,42]. It allows to examine in detail various design aspects and parameters and to develop a better design [43] as well as to perform optimization [44–46]. Certain problems, like those in fluid dynamics, are complex and require virtual prototype validation, and an approach that uses a combination of virtual and physical prototyping gives a good way to solve them [47].

The presented study aims to develop a new hydrokinetic system, using a validated virtual prototype of a crossflow turbine. The virtual prototype is used to perform numerical

simulations to assess a concept for a crossflow turbine, Bánki–Michell/Ossberger (BMO) type, with a vertical-axis design for river applications. The final target is to obtain an overall evaluation of the possible application of such a hydrokinetic system in big rivers, with high level of water discharge. This evaluation is directed to obtain the possible generated power, and the technical feasibility of this type of solution. The novelty of the presented study is related to the in-stream application of a vertical (instead of horizontal) axis BMO turbine that is evaluated through virtual prototyping, because of its relatively large size.

2. Materials and Methods

Crossflow turbines are studied for their application as in-stream installations, predominantly as horizontal-axis turbines [48–50]. Vertical-axis turbines of various types are also examined [51,52], but the Bánki–Michell/Ossberger type is not in focus. BMO type is a very efficient and economical choice that allows a very good price/performance ratio. Its efficiency is a little less than a Kaplan, Francis, or Pelton turbine, but it maintains high efficiency values within a large range, specially above the optimum discharge value. BMO turbine design is explored widely and some parameters are outlined as important. The angle between the particles trajectories along the circumference of the impeller inlet and the tangent to the same circumference is one of these parameters [32]. Further examination is focused exactly on this type of hydrokinetic system, applied in a big river environment.

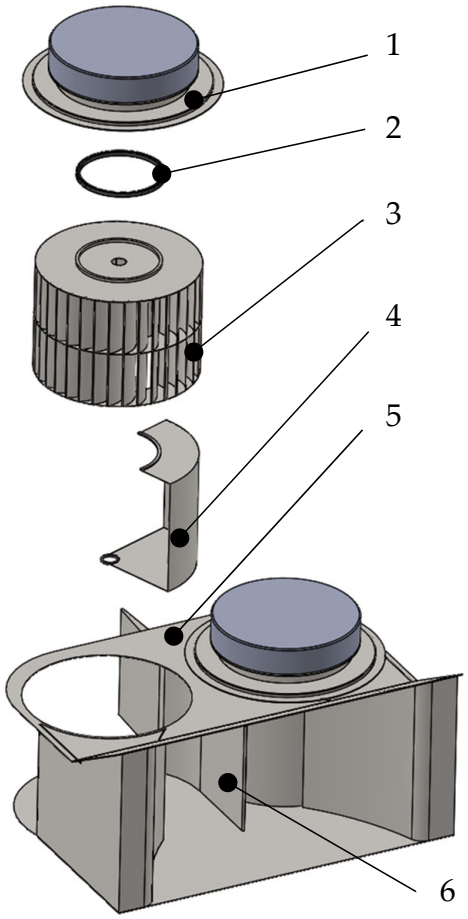
2.1. The Site

An important point in each implementation is the potential site of a certain technology application. This study refers to a river site with relatively high fluid flow. This hydrokinetic system is planned to operate over a wide range of ambient river flows, including high discharge and low gradient. For maximizing power production, the system can be installed in a dedicated derivation channel, where water velocity is accelerated locally before reaching the turbine blades. General channel requirements are related to width: 30–40 m; depth: 3–6 m; and length from >500 m to 2 km.

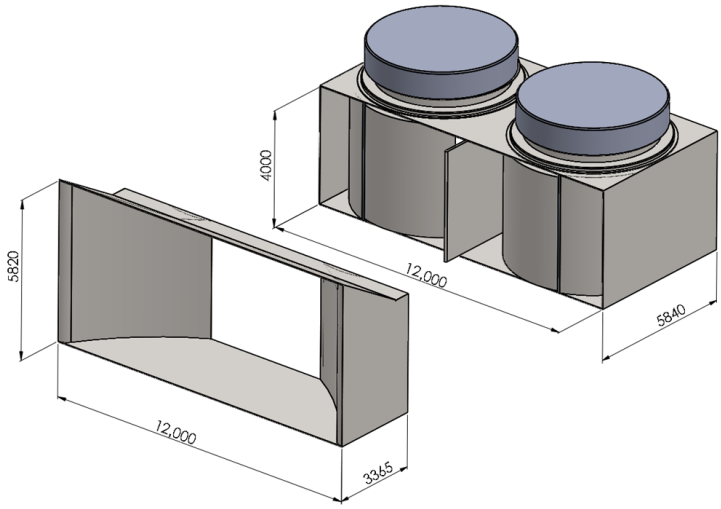
Other important starting characteristics, concerning the river, are minimum discharge > 200 m^3/s; average discharge > 400 m^3/s; and mid-range gradient: >1:50. These values guarantee a high amount of harvested energy and are a good solution for developing regions. Preferences for the location on the river should be downstream of a dam where outflow discharge is controlled to avoid the seasonal dry periods with the lowest discharges. These conditions are available in Europe for a few rivers like Danube and Rhine [53], as well as in Asia [54]. Such an example is the Mekong river in Southeast Asia, flowing through China, Myanmar, Laos, Thailand, Cambodia, and Vietnam. It reaches maximal discharge of more than 23,500 m^3/s [55].

2.2. The Concept

The main point in this concept is to use BMO turbine with vertical axis. The reference point for vertical axis use is to simplify the design and to obtain a good price/performance value of the installation. The vertical axis gives good opportunities to separate the turbine from the rest of the system easily, enabling easy sealing of the external components like the generator and the support system. This separation is important for the mechanical design of the system and benefits specifically by the vertical installation of the turbine. Crossflow (BMO) device concept is shown in Figure 1, in principle.



(**a**) Explode view



Design parameters

crossflow turbine wheel diameter:	5.6 m
crossflow turbine wheel height:	5.2 m
crossflow turbine wheel blades no:	35
turbines centre distance:	5.9 m

Installation site parameters

minimum discharge:	200 m^3/s
average discharge:	400 m^3/s
mid-range gradient:	1:50

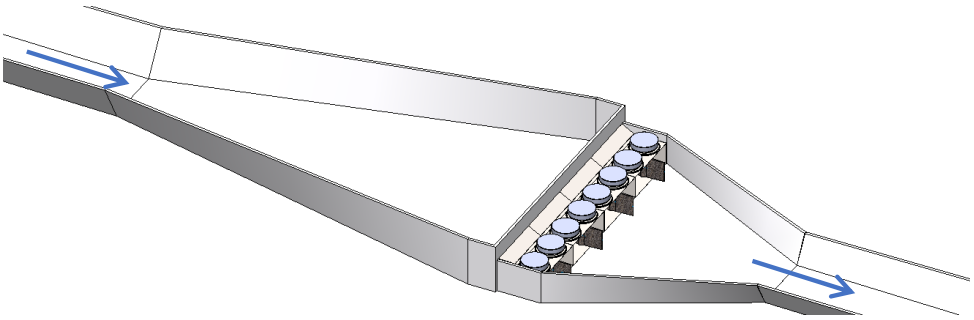
(**b**) Overall dimensions, mm

Figure 1. Conceptual design of Bánki–Michell/Ossberger turbine module.

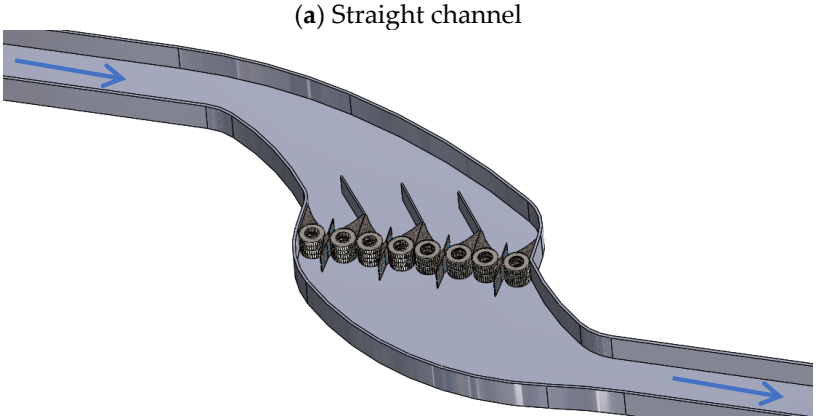
The hydrokinetic unit comprise two sub modules, and each of them has separate turbine (pos. 3), connected to a generator (pos. 1), carried by a bearing subsystem (pos. 2), in a housing (pos. 5). The flow is planned to be controlled by a rotational shield (pos. 4)—for each turbine separately. The vertical wall (pos. 6) is used to guide the flow, forming a nozzle, and to obtain near to optimal output parameters. The crossflow turbine wheel is of 5.6 m diameter and 5.2 m height, having 35 blades, with overall dimensions of the module, as it is shown in Figure 1b.

The above-described module could be used for different combinations, depending on the channel and its specifics. Possible variants are shown in Figure 2.

The channel and installation specifics require a head of 6 m, and this head corresponds to 300 m length for slope 1:50 (or 600 m length for slope 1:100). The major difference between the two channel design variants is that the curved channel (Figure 2b is more compact in length when compared to straight channel (the turbine station length is about 80 m for curved channel and about 130 m for the straight channel). Total length, at 1:50 slope, for one station of BMO modules is 380 m, or 1900 m for five stations. More detailed design parameters of the channels are to be defined in a further design development stage.



(**a**) Straight channel



(**b**) Curved channel

Figure 2. Conceptual variants for BMO modules placement in different channels (arrows are showing the water flow direction).

2.3. The Virtual Prototype

A virtual prototype of the above discussed system is developed. The target is to evaluate the design performance as to obtain concept assessment before proceeding with design details. This prototype is built according to the specifics of the simulation tool to be used—ANSYS Fluent software 2019 R3 —commercially available general-purpose Computational Fluid Dynamics (CFD) code for simulation of fluid flow, heat, and mass transfer. It is based on finite volume method as a numerical technique and provides sufficient accuracy when simulating turbulent currents.

Planned simulations involve 3D modelling and sliding mesh (a technique for simulating relative motion between fluid domains by using a non-conformal mesh, using interpolation between disconnected mesh regions). Sliding mesh also requires an adequate time discretization, as the node displacement per time step on the outer boundary of the sliding mesh must be less than (or equal to) the element mesh size. A simulation model is built, based on virtual prototype. Its geometry is shown in Figure 3, where only the fluid domain is presented. The model uses available geometry and boundary conditions symmetry and presents the half of modelled BMO turbines module. Special attention is paid to the rotating turbine volume, where an external thin ring is used as an interface region. It rotates with the turbine region and the contact to the static mesh is planned to be on its external surface.

A 3D numerical model is presented in Figure 4 to present the mesh density and characteristics. It contains approximately 372,000 cells (hexagonal type) and 412,000 nodes. The generated mesh has sufficient quality (skewness is less than 0.5) to perform a dynamics simulation (sliding mesh) and to achieve good convergence and result accuracy, without influencing the output parameters (grid-independence analysis is obtained, based on prior experience, reported in [56]). The mesh is denser in the blade region (20 cells along the blade) to capture gradients in the flow parameters with sufficient accuracy, providing a

good transfer to the static region. This quality is possible and achievable mainly because of the "sweepable" geometry, which is also suitable for 2D modelling. The simulation is performed using a 3D model rather than a 2D model, to allow future simulations to model partial water filling of the turbine volume. This is not a subject in the presented research but is planned for future studies.

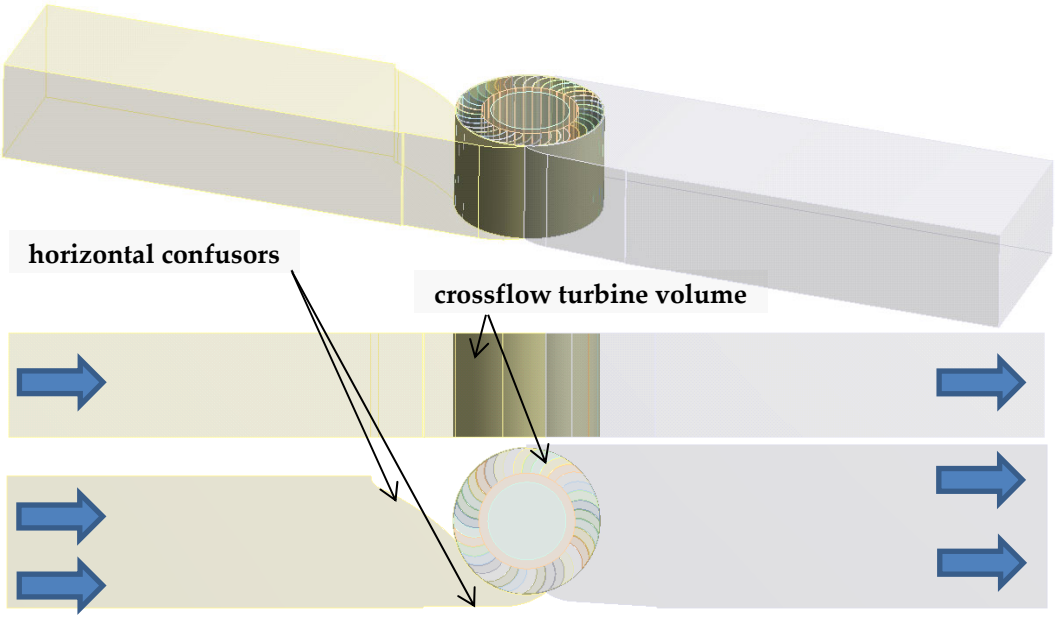


Figure 3. Geometry of examined BMO module, used for simulations.

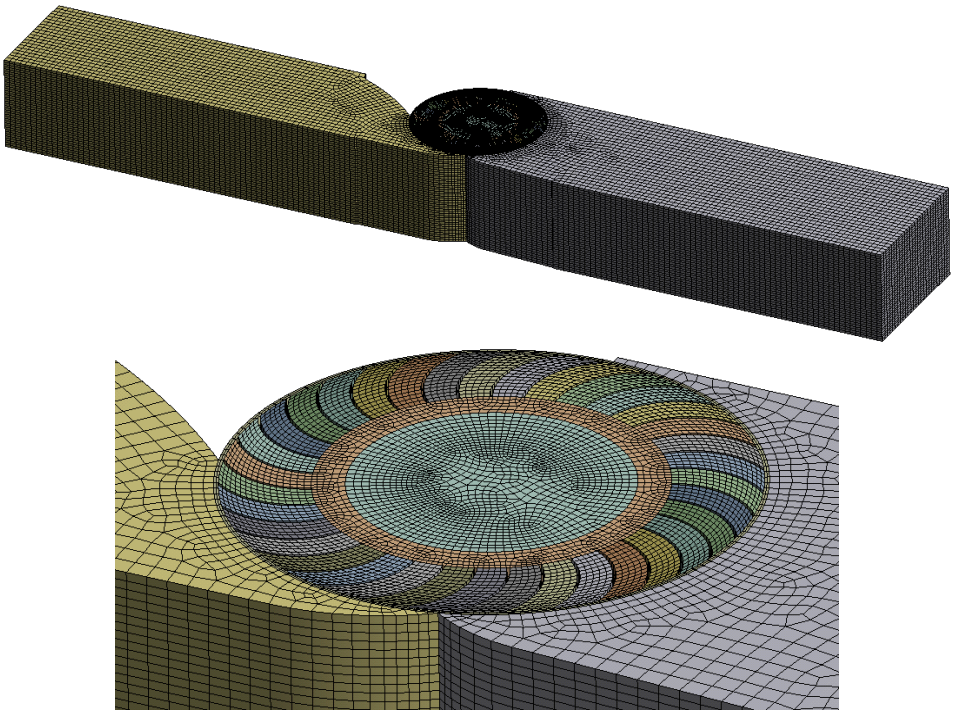


Figure 4. Three-dimensional mesh model of crossflow turbines design.

Applied boundary conditions (BCs) in the 3D model assume a fully submerged turbine with no air inclusions, with the entire model consisting of water. Crossflow turbine volume is defined as a dynamic, rotating mesh, having an interface with the near stationary fluid volume. Its angular velocity is defined for each analysis separately. General presentation of

the applied boundary conditions is shown in Figure 5. The applied boundary conditions are specified as follows:

- Inlet BCs:
  - 4 modules are planned for installation at a station, as discussed in Section 2.2;
  - The average value of water discharge is used for this model, with a value as defined in Section 2.1—400 m^3/s;
  - The inlet velocity represents a volumetric flow of 100 m^3/s, which is a quarter (4 modules) of the total discharge.
- Outlet BCs:
  - Pressure outlet boundary condition is defined at the opposite end of the modelled domain. The gauge pressure is set to zero.
- Turbine volume:
  - The rotational speed is set for the separate volumes of the turbine blades and their surroundings. It varies across simulations to obtain a full characterization of the examined system.

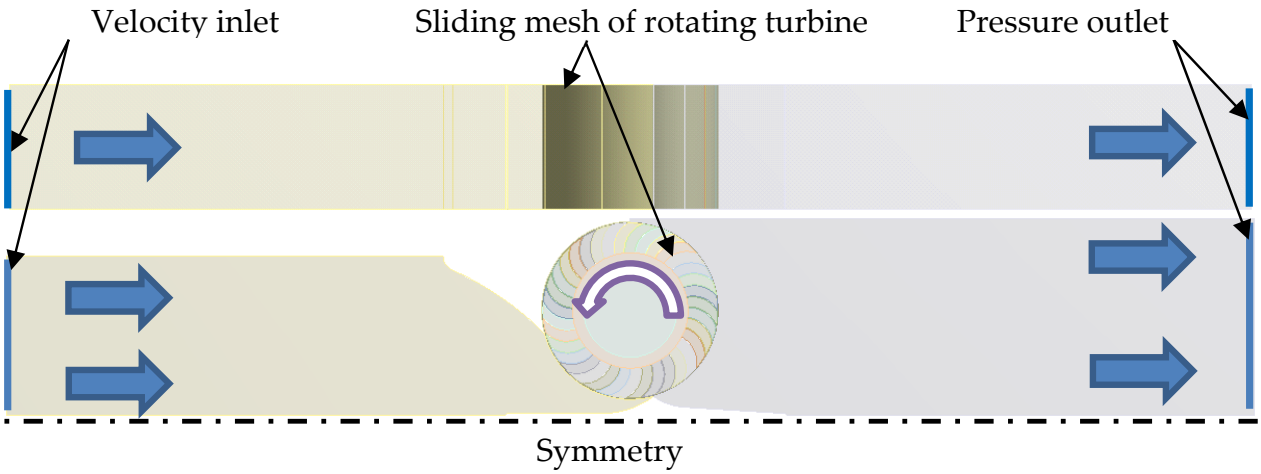


Figure 5. Applied boundary conditions.

The numerical simulation was performed based on Reynolds averaged Navier–Stokes equations with k-ε turbulence model, which gives a general description of turbulence by means of two transport equations. The pressure-based solver with absolute velocity formulation was used, with gravity and axis of rotation in the vertical z direction considered. The fluid considered was water with x-axis flow direction, and density 998.2 kg/m^3, and viscosity 0.001003 kg/m·s. The residuals—the imbalance in the physical conservation equations (mass, momentum, energy, etc.)—are set to 10^{-6}.

Performed simulations aimed to determine the characteristics of the examined system in terms of output mechanical power and efficiency, at different rotational speed values for the turbine. These characteristics correspond to the system performance at different active loads (rotational speed). Obtaining these curves requires running several simulations to extract response values for generated power and the efficiency of the examined system. The output mechanical power is calculated from the mechanical torque measured in the simulation model, acting on the turbine blades, corresponding to a certain angular velocity:

$$P_T = T * \omega_T = \frac{\pi \cdot T \cdot n_T}{30} \quad (1)$$

where

T—torque, generated over the turbine blades;

ω_T—angular velocity of the turbine volume (input boundary condition), rad/s;

n_T—rotational speed of the turbine volume, 1/min.

The efficiency is determined as the proportion between hydraulic power and gained by the turbine power as follows:

$$\eta = \frac{P_T}{P_F} \quad (2)$$

where

P_F—hydraulic power of the inlet fluid (the product of the fluid's pressure and its volumetric flow rate), simplified and calculated as follows:

$$P_F = Q * \Delta p \quad (3)$$

where

Q—volumetric flow rate, m^3/s (input boundary condition through the applied inlet velocity V_{in});

Δp—total pressure difference, determined by performed CFD simulation.

Thus, the following parameters are derived from the simulation model directly: torque T, total pressure p, while the following parameters are input for the model: inlet velocity V_{in} and angular velocity ω_T.

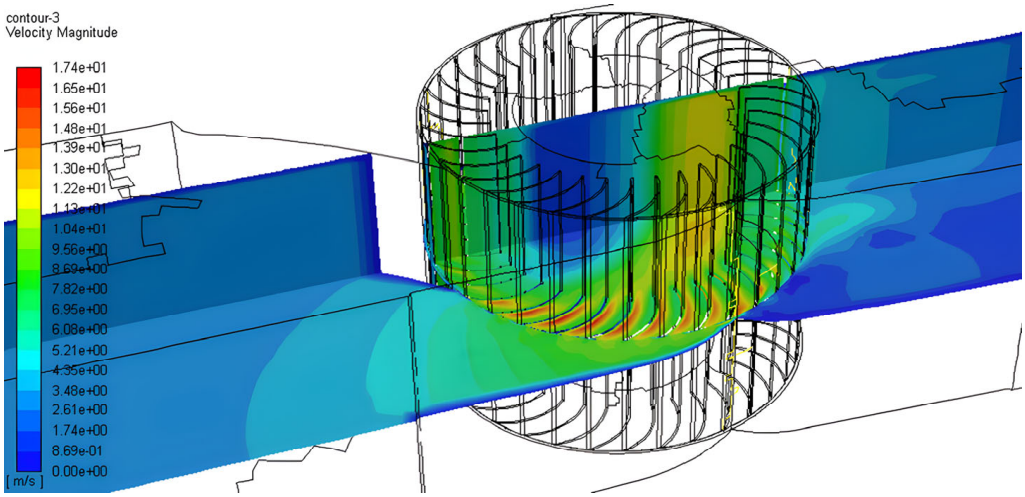
Prepared virtual prototype is validated through a separate simulation that is performed using the design and geometry of a physical prototype. This physical prototype is downscaled (external turbine diameter is 246 mm), with kept proportions of the entire system, which allows easy testing in an open channel stand, available in the research facilities. This physical prototype is not directly comparable to the one studied in this research system, but its virtual prototype is relevant. The results from the performed tests over this downscaled physical prototype, used for the virtual prototype validation, are reported in a previous study [56]. The validation is performed through a comparison of the physical prototype results against the simulation results, obtained using a virtual prototype of tested turbine. It is not especially presented in this study, as it was studied in a separate study, where the data from physical tests are used [56]. Performed validation is used to adjust the virtual prototype in the analysis setup, such as selecting a suitable turbulence model (k-ε) and its parameters. Adjustments are also for other solution-specific details, such as selecting appropriate solution methods for pressure–velocity coupling, spatial discretization, and control parameter values (relaxation). The obtained results from the adjusted virtual prototype of downscaled BMO are finally compared with physical prototype measurements, and the overall approach is validated. The defined output parameters for blade torque calculation and inlet total pressure are used to assess solution convergence.

3. Results

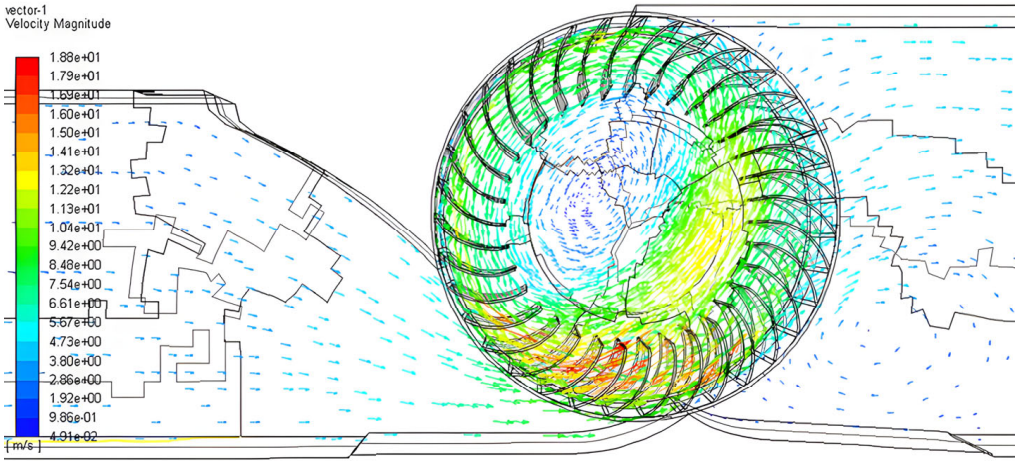
3.1. Results Overview

Obtained results are presented, in general, for one of the performed at different rotational speed simulations, to present some parameters of interest.

The results are initially presented by velocity magnitude distribution field (Figure 6a) and by velocity vectors (Figure 6b). This presentation is used mainly to assess overall results, and the velocity shows maximal value of about 18 m/s. Low-velocity regions are observed (just after the turbine and at the centre), especially after the turbine, suggesting opportunities for further performance optimization. The so-called "two-pass" flow is seen, especially in Figure 6b, where the flow is seen to pass diagonally through the turbine wheel.



(**a**) Magnitude distribution field in two perpendicular cross sections



(**b**) Vectors in a longitudinal cross section

Figure 6. Velocity presentation, m/s.

The total pressure distribution field is shown in Figure 7, where the high-pressure path, indicating the flow direction, is clearly visible. The velocity and pressure distributions indicate that the obtained data are sufficient to assess the system's output parameters. These results are used to calculate the inlet total pressure, which is then used to determine the inlet flow power. This value, together with the torque, generated over turbine blades, is also used as an indicative parameter to check the solution convergence during the simulation run.

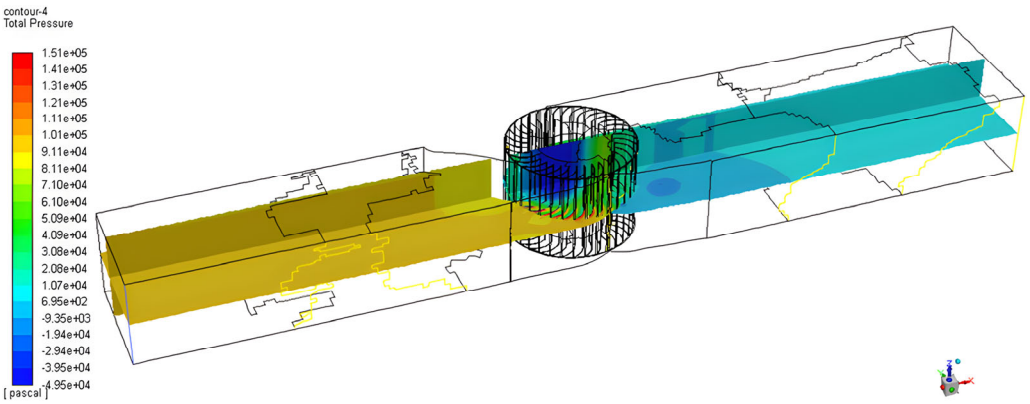
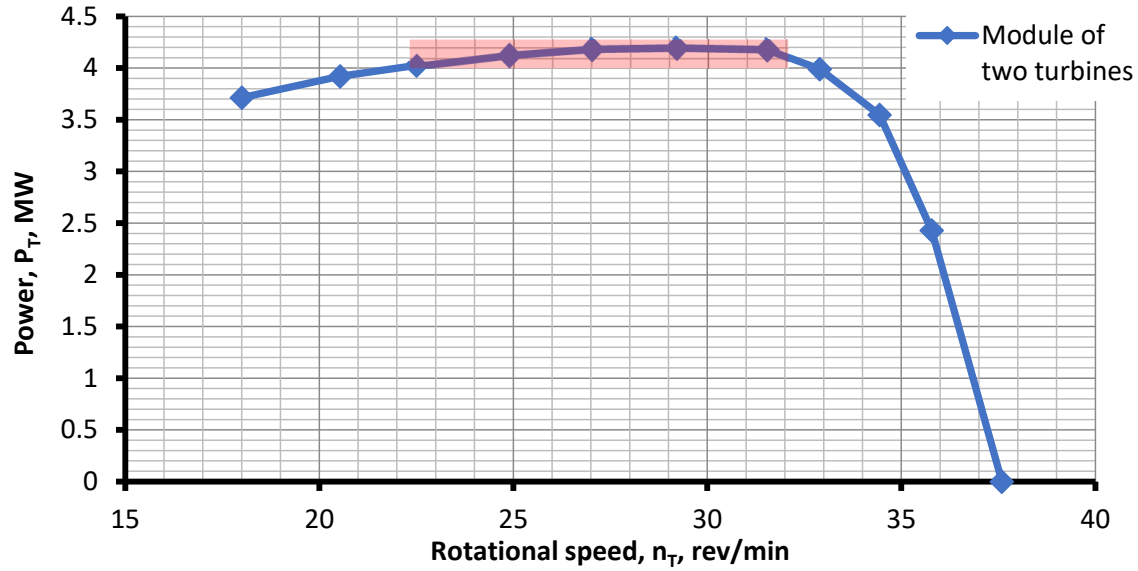


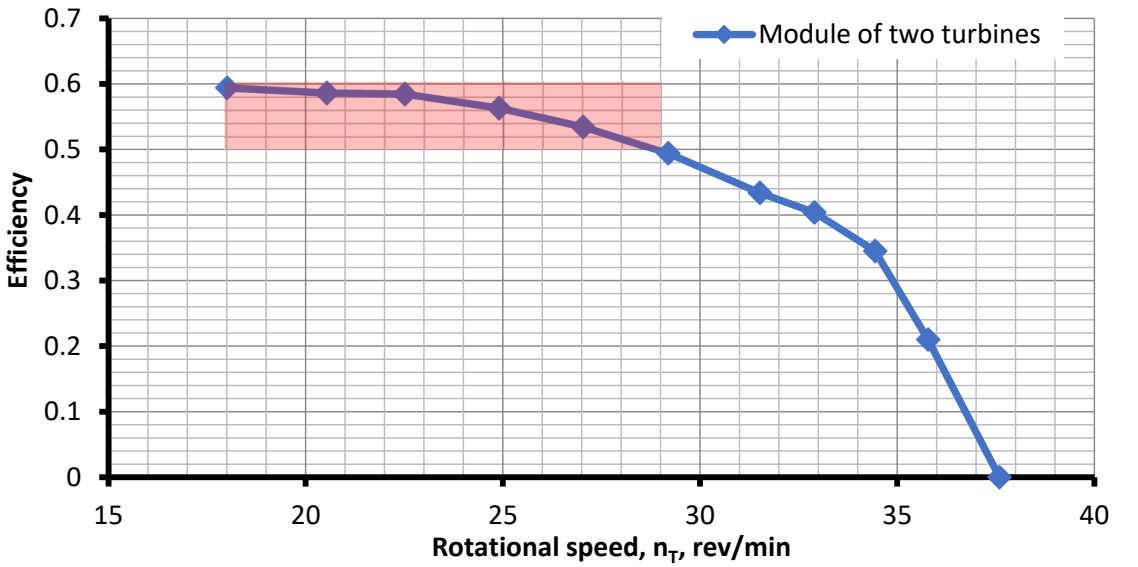
Figure 7. Total pressure distribution field in two perpendicular cross sections, Pa.

3.2. Turbine Characteristics

Next, the following two parameters of turbine performance are presented: the generated power (mechanical power) and the efficiency. Eleven separate simulations are run, varying the turbine volume's rotational speed. The moment (mechanical torque) acting on the blades is calculated by the software and stored as a separate parameter in the database. The obtained mechanical torque results are used to calculate the power generated by the turbine blades. Efficiency is calculated using the equations shown above ((1)–(3)). Determined parameters are shown as functions of the rotational speed in Figure 8.



(**a**) Power generated for both turbines at different rotational speed.



(**b**) Efficiency at different rotational speed.

Figure 8. System parameters at different rotational speed.

Several comments could be formed:

- Crossflow turbine performance is stable in a relatively wide rotational speed range (marked in red zone in Figure 8)—it generates power higher than 4 MW in the range from 22.5 min^{-1} to 32 min^{-1};
- Obtained maximal efficiency of about 60% is in the expected range for such type of turbines—20÷80% [13,32,57];

- There is potential for further improving efficiency, primarily through a detailed study of the number of turbine blades, geometry, and the diffuser. Such studies exist and the ways to improve the performance are well-studied [34,58,59];
- The efficiency decreases with an increase in rotational velocity, but harvested energy increases, as well as the required head;
- Rotational speed over 35 min^{-1} is inefficient;
- A good solution is to operate at 29 min^{-1}, where the power is nearly 4.2 MW and the efficiency is about 50%;
- Total power generation by a site station on the channel, where four modules are installed, is equal to 16.8 MW;
- Planned distance of 1900 m, with five site stations, will be capable to generate 84 MW power.

4. Discussion

The proposed concept that uses a crossflow turbine with vertical axis for an in-stream application in river with high discharge is studied in two aspects—technical feasibility and financial aspect.

4.1. Technical Aspect

The performed study shows a practical application of approach for product development that is based on virtual prototyping, with preliminary validation of downscaled physical prototype. Virtual prototyping simulations show a good performance—with calculated 4.2 MW generation power for the examined crossflow turbine, or 16.8 MW for an installation site with four modules installed, or overall production of about 0.7 TWh per year (at 400 m^3/s water discharge). The generated power could be maintained in a relatively wide range of conditions (rotational speed of the turbine). The efficiency of 50–60% provides a perspective for further concept development at the stage of detailed design development. Used virtual prototyping gives options for easy design changes and evaluation, which is a good basis for the improvement of the system performance.

The proposed concept for in-stream power generation will require a separate channel in parallel with the river, which is a viable alternative to conventional dam structures. The potential for in-stream turbines is high, and site-specific optimization of turbine array arrangements could enhance their suitability and support sustainable hydropower development in regions such as Mainland Southeast Asia. Further development would require a detailed design development to assess different sides of the project, related to mechanical structure, electrical components (generator, inverter), and a detailed assessment of environmental aspects (related to a certain region).

4.2. Financial Aspect

The obtained results show a good perspective for application of this concept in rivers with high average discharge. The calculated value for generated power in a 1.9 km distance is 84 MW, which gives about 0.7 TWh per year, for 400 m^3/s water discharge. This is a viable solution that could contribute to the regional electricity production, especially in countries with sufficient hydro energy technical potential. Available data for 2020 show that hydroelectricity generation is developed in Europe (close to 50% of technical potential), while Asia (24%) and Africa (6%) have good perspectives [60]. Studies show that Asia has the largest potential (8160 TWh/y) and only 25% is utilized [61].

In recent years, hydroelectricity generation has increased (from 2020 to 2024 by about 70%) [62], indicating increased interest in investment. Generally, the electrical

energy generated by hydro sources has a Levelized Cost of Energy in the range of 0.01–0.9 US $/kWh [63,64], which is comparable to that of fossil fuels.

Preliminary studies over the cost of the presented concept show that the capital expenditure cost (CAPEX) is expected to reach $109 million (for five sites with four modules of two turbines each), civil works ($14 million), power infrastructure ($5.3 million), and project development cost ($6.6 million). The generated income per year (for 80 US $/MWh), at average water discharge of 400 m^3/s, is calculated as $56.5 million, which shows return of investment (ROI) varying between 2 (for average water discharge) and 4.5 years, depending on the averaged discharge of the river. The maximal calculated value of 4.5 years is for 150 m^3/s discharge, which is the lower boundary for this conceptual design. This is a typical value for a hydropower unit, with investment cost up to 8400 $/kW [65].

5. Conclusions

A summary of the performed study shows that the evaluated concept is applicable, especially for rivers with high level of discharge, with a perspective ROI. The evaluation shows a potential to harvest 84 MW at the average water discharge level of 400 m^3/s, resulting in 2 years' return of investment (0.7 TWh per year). Further examinations for a detailed design development should be preceded by a detailed business plan for a certain site of installation. Another important option is to perform design optimization and to improve the efficiency of the system.

Presented study also demonstrates the advantages of virtual prototyping when it is applied at early design development stage—concept evaluation. The validation of a downscaled model gives sufficient confidence of the obtained for the larger structure results. The virtual prototyping provides opportunity to assess a relatively large structure and decrease significantly the product development expenses by eliminating the need of physical prototyping and testing. Developed simulation model is a basis also for further design improvement and will be used in future studies.

Author Contributions: Conceptualization, G.T., K.K. and R.M.; methodology, K.K., G.T. and R.M.; software, K.K. and T.I.; validation, T.I. and K.K.; formal analysis, G.T.; investigation, K.K. and T.I.; resources, T.I. and R.M.; data curation, R.M. and T.I.; writing—original draft preparation, K.K.; writing—review and editing, G.T. and K.K.; visualization, T.I. and R.M.; supervision, G.T.; project administration, G.T. and R.M.; funding acquisition, G.T. and K.K. All authors have read and agreed to the published version of the manuscript.

Funding: This work was supported by European Regional Development Fund under "Research Innovation and Digitization for Smart Transformation" programme 2021–2027 under the Project BG16RFPR002-1.014-0006 "National Centre of Excellence Mechatronics and Clean Technologies", and by the project КП-06-Н67/8 "Development of a fluid-structural methodology for the study and modernization of HYDRAulic turbomachines, through the TECHnologies of virtual prototyping–HydraTech".

Data Availability Statement: The original contributions presented in this study are included in the article. Further inquiries can be directed to the corresponding author.

Conflicts of Interest: The authors declare no conflict of interest.

Abbreviations

The following abbreviations are used in this manuscript:

BMO	Bánki–Michell/Ossberger
CFD	Directory of open access journals
CAPEX	Capital expenditure cost
BCs	Boundary conditions
ROI	Return of investment

References

1. Norrman, K.-E. World Population Growth: A Once and Future Global Concern. *World* **2023**, *4*, 684–697. [CrossRef]
2. Hickel, J.; Sullivan, D. How much growth is required to achieve good lives for all? Insights from needs-based analysis. *World Dev. Perspect.* **2024**, *35*, 100612. [CrossRef]
3. Sharma, V.K.; Monteleone, G.; Braccio, G.; Anyanwu, C.N.; Aneke, N.N. A Comprehensive Review of Green Energy Technologies: Towards Sustainable Clean Energy Transition and Global Net-Zero Carbon Emissions. *Processes* **2025**, *13*, 69. [CrossRef]
4. Bhatt, K.; Kumar, S.; Kumar, S.; Sharma, S.; Singh, V. A review on energy harvesting technologies: Comparison between non-conventional and conceptual approaches. *Energy Rep.* **2024**, *12*, 4717–4740. [CrossRef]
5. Suh, Y.H.; Wang, C.; Chang, K. Circularly polarised truncated-corner square patch microstrip rectenna for wireless power transmission. *Electron. Lett.* **2000**, *36*, 600–602. [CrossRef]
6. Maradin, D. Advantages and disadvantages of renewable energy sources. *Int. J. Energy Econ. Policy* **2021**, *11*, 176–183. [CrossRef]
7. Kabeyi, M.J.; Olanrewaju, O. Wind Energy in Sustainable Power Generation and Supply. In Proceedings of the 2nd Australian International Conference on Industrial Engineering and Operations Management, Melbourne, Australia, 14 May 2023.
8. Alabdali, Q.A.; Bajawi, A.B.; Fatani, A.M.; Nahhas, A.M. Review of Recent Advances of Wind Energy. *Sustain. Energy* **2020**, *8*, 12–19.
9. Nwankwo, C.; Lele, D. Comprehensive analysis of advancements in wind turbine design and offshore wind energy integration: Technological innovations, economic viability, and environmental impacts. *Int. J. Appl. Res. Soc. Sci.* **2024**, *6*, 1538–1556. [CrossRef]
10. Jung, C. Recent Development and Future Perspective of Wind Power Generation. *Energies* **2024**, *17*, 5391. [CrossRef]
11. Iliev, R.; Tsalov, T. Investigation of a cross-flow wind turbine with a hybrid frontal guiding device. *IOP Conf. Ser. Earth Environ. Sci.* **2024**, *1380*, 012001. [CrossRef]
12. Yuce, M.I.; Muratoglu, A. Hydrokinetic energy conversion systems: A technology status review. *Renew. Sustain. Energy Rev.* **2015**, *43*, 72–82. [CrossRef]
13. Tesfay, A.H.; Weldemariam, S.A.; Gebrelibanos, K.G. Design and Development of Crossflow Turbine for Off-Grid Electrification. *Energies* **2025**, *18*, 5108. [CrossRef]
14. Elbatran, A.H.; Abdel-Hamed, M.W.; Yaakob, O.B.; Ahmed, Y.M.; Ismail, M.A. Hydro Power and Turbine Systems Reviews. *J. Teknol. (Sci. Eng.)* **2015**, *74*, 83–90. [CrossRef]
15. Khan, M.; Bhuyan, G.; Iqbal, M.; Quaicoe, J. Hydrokinetic Energy Conversion Systems and Assessment of Horizontal and Vertical Axis Turbines for River and Ridal Applications: A Technology Status Review. *Appl. Energy* **2009**, *2*, 1823–1835. [CrossRef]
16. Niebuhr, C.M.; van Dijk, M.; Neary, V.S.; Bhagwan, J.N. A review of hydrokinetic turbines and enhancement techniques for canal installations: Technology, applicability and potential. *Renew. Sustain. Energy Rev.* **2019**, *113*, 109240. [CrossRef]
17. Coban, H.H. Hydropower Planning in Combination with Batteries and Solar Energy. *Sustainability* **2023**, *15*, 10002. [CrossRef]
18. Prajwal, G.; Quaranta, E.; Coronado, O.; Ramos, H. Hydropower Advantages over Batteries in Energy Storage of Off-Grid Systems. *Energies* **2023**, *16*, 6309. [CrossRef]
19. Zhou, D.; Deng, Z.D. Ultra-low-head hydroelectric technology: A review. *Renew. Sustain. Energy Rev.* **2017**, *78*, 23–30. [CrossRef]
20. Kougias, I.; Aggidis, G.; Avellan, F.; Deniz, S.; Lundin, U.; Moro, A.; Muntean, S.; Novara, D.; Perez-Díaz, J.I.; Quaranta, E.; et al. Analysis of emerging technologies in the hydropower sector. *Renew. Sustain. Energy Rev.* **2019**, *113*, 109257. [CrossRef]
21. Muller, G.; Kauppert, K. Performance characteristics of water wheels. *J. Hydraul. Res.* **2004**, *42*, 451–460. [CrossRef]
22. Quaranta, E.; Muller, G. Optimization of undershot water wheels in very low and variable flow rate. *J. Hydraul. Res.* **2020**, *58*, 845–849. [CrossRef]
23. Quaranta, E. Stream water wheels as renewable energy supply in flowing water: Theoretical considerations, performance assessment and design recommendations. *Energy Sustain. Dev.* **2018**, *45*, 96–109. [CrossRef]
24. Quaranta, E.; Revelli, M. Gravity water wheels as a micro hydropower energy source: A review based on historic data, design methods, efficiencies and modern optimizations. *Renew. Sustain. Energy Rev.* **2018**, *97*, 414–427. [CrossRef]
25. Quaranta, E.; Bahreini, A.; Riasi, A.; Revelli, R. The very low head turbine for hydropower generation in existing hydraulic infrastructures: State of the art and future challenges. *Sustain. Energy Technol. Assess.* **2022**, *51*, 101924. [CrossRef]
26. Riglin, J.; Daskiran, C.; Jonas, J.; Schleicher, W.C. Hydrokinetic turbine array characteristics for river applications and spatially restricted flows. *Renew. Energy* **2016**, *97*, 274–283. [CrossRef]
27. Chica, E.; Rubio-Clemente, A. Design of Zero Head Turbines for Power Generation. In *Renewable Hydropower Technologies*; IntechOpen: London, UK, 2017; pp. 25–50.
28. Gandhi, J.R.; Jha, H.; Jha, S.N.; Patel, D.S. Renewable Energy Based Floating Power Generator (Rivers and Canals). *Int. J. Eng. Res. App.* **2016**, *6*, 49–52.
29. Huertas-Hernando, D.; Farahmand, H.; Holttinen, H.; Kiviluoma, J.; Rinne, E.; Söder, L.; Menemenlis, N. Hydro power flexibility for power systems with variable renewable energy sources: An IEA Task 25 collaboration. In *Advances in Energy Systems: The Large-Scale Renewable Energy Integration Challenge, WIREs Energy and Environment*; Wiley Online: Hoboken, NJ, USA, 2017; pp. 240–263.
30. Muljadi, E.; Wright, A.; Gevorgian, V.; Donegan, J.; Marnagh, C.; McEntee, J. *Power Generation for River and Tidal Generators*; National Renewable Energy Laboratory: Golden, CO, USA, 2016.

31. Laws, N.D.; Epps, B.P. Hydrokinetic energy conversion: Technology, research and outlook. *Renew. Sustain. Energy Rev.* **2016**, *57*, 1245–1259. [CrossRef]
32. Sinagra, M.; Sammartano, V.; Aricòa, C.; Collura, A.; Tucciarelli, T. Cross-Flow turbine design for variable operating conditions. In Proceedings of the 12th International Conference on Computing and Control for the Water Industry, CCWI2013, Perugia, Italy, 2–4 September 2013; pp. 158–172.
33. Behrouzi, F.; Maimun, A.; Nakisa, M. Review of Various Designs and Development in Hydropower Turbines. *Int. J. Mech. Aerosp. Ind. Mechatron. Manuf. Eng.* **2014**, *8*, 293–297.
34. Adhikari, R.; Wood, D. The Design of High Efficiency Crossflow Hydro. *Energies* **2018**, *11*, 353–362. [CrossRef]
35. Cunden, K.; Inambao, F. Numerical Simulation of a Vertical Axis Crossflow Helical Hydrokinetic Turbine. *J. Propuls. Technol.* **2024**, *45*, 6265–6284.
36. Zouzou, B.; Dobrev, I.; Massouh, F.; Dizene, R. Experimental and numerical analysis of a novel Darrieus rotor with variable pitch mechanism at low TSR. *Energy* **2019**, *186*, 115832. [CrossRef]
37. Quaranta, E.; Revelli, M. CFD simulations to optimize the blade design of water wheels. *Drink. Water Eng. Sci.* **2017**, *10*, 27–32. [CrossRef]
38. Tian, W.; Mao, Z.; Ding, H. Design, test and numerical simulation of a low-speed horizontal axis. *Int. J. Nav. Archit. Ocean. Eng.* **2018**, *10*, 782–793. [CrossRef]
39. Mrope, H.; Jande, Y.; Kivevele, T. A Review on Computational Fluid Dynamics Applications in the Design and Optimization of Crossflow Hydro Turbines. *J. Renew. Energy* **2021**, *10*, 5570848. [CrossRef]
40. Bodner, C.; Benigni, H.; Jaberg, H. Development of a Cross-Flow Turbine by using 3D-CFD-Calculations. In Proceedings of the 17th International Conference on Fluid Flow Technologies, Budapest, Hungary, 4–7 September 2018.
41. Wang, G. Definition and Review of Virtual Prototyping. *J. Comput. Inf. Sci. Eng.* **2002**, *3*, 232–236. [CrossRef]
42. Chu, C.-H.; Kao, E.-T. A Comparative Study of Design Evaluation with Virtual Prototypes Versus a Physical Product. *Appl. Sci.* **2020**, *10*, 4723. [CrossRef]
43. Todorov, G.D.; Kamberov, K.H. Black box/white box hybrid method for virtual prototyping validation of multiphysics simulations and testing. *IOP Conf. Ser. Mater. Sci. Eng.* **2020**, *878*, 012051. [CrossRef]
44. Zheng, X.; Zhao, Y.; Zhang, H.; Pu, Y.; Li, Z.; Guo, P. Optimization and Performance Analysis of Francis Turbine Runner Based on Super-Transfer Approximate Method under Multi-Energy Complementary Conditions. *Sustainability* **2022**, *14*, 10331. [CrossRef]
45. Peng, X.; Zhou, J.; Zhang, C.; Li, R.; Xu, Y.; Chen, D. An Intelligent Optimization Method for Vortex-Induced Vibration Reducing and Performance Improving in a Large Francis Turbine. *Energies* **2017**, *10*, 1901. [CrossRef]
46. Malakov, I.; Zaharinov, V. Optimization of size ranges of technical products. *Appl. Mech. Mater.* **2016**, *859*, 194–203. [CrossRef]
47. Liu, B. *Integration of Physical and Virtual Prototyping*; Loughborough University: Loughborough, UK, 2011.
48. Picone, C.; Sinagra, M.; Gurnari, L.; Tucciarelli, T.; Filianoti, P. A New Cross-Flow Type Turbine for Ultra-Low Head in Streams and Channels. *Water* **2023**, *15*, 973. [CrossRef]
49. Picone, C.; Sinagra, M.; Tucciarelli, T. A new regulation system for Crossflow type turbines for water management industry. *Energy* **2025**, *328*, 136695. [CrossRef]
50. Anand, R.S.; Jawahar, C.; Bellos, E.; Malmquist, A. A comprehensive review on Crossflow turbine for hydropower applications. *Ocean Eng.* **2021**, *240*, 110015. [CrossRef]
51. Karakaya, D.; Bor, A.; Elçi, S. Numerical Analysis of Three Vertical Axis Turbine Designs for Improved Water Energy Efficiency. *Energies* **2024**, *17*, 1398. [CrossRef]
52. Zanette, J.; Imbault, D.; Tourabi, A. A design methodology for cross flow water turbines. *Renew. Energy* **2010**, *35*, 997–1009. [CrossRef]
53. Santos, I.M.; Herrnegger, M.; Holzmann, H. Seasonal discharge forecasting for the Upper Danube. *J. Hydrol. Reg. Stud.* **2021**, *37*, 100905. [CrossRef]
54. Lu, X.X.; Chua, S. River Discharge and Water Level Changes in the Mekong River: Droughts in an Era of Mega-Dams. *Hydrol. Process.* **2021**, *35*, 1002. [CrossRef]
55. Pawar, U.; Sophal, T.; Muttil, N.; Rathnayake, U.; Suppawimut, W. Frequency and trend analyses of annual peak discharges in the Lower Mekong Basin. *Heliyon* **2023**, *9*, e19690. [CrossRef]
56. Todorov, G.; Obretenov, V.; Kamberov, K.; Ivanov, T.; Tsalov, T.; Zlatev, B. Concept and Physical Prototyping of Micro Hydropower System Using Vertical Crossflow Turbine. In Proceedings of the 2021 6th International Symposium on Environment-Friendly Energies and Applications, EFEA 2021, Sofia, Bulgaria, 11–14 May 2021.
57. Anurag, K.; Saini, R.P. Development of Hydrokinetic Power Generation System: A Review. *Int. J. Eng. Sci. Adv. Technol.* **2014**, *4*, 464–477.
58. Sammartano, V.; Aricò, C.; Carravetta, A.; Fecarotta, O.; Tucciarelli, T. Banki-Michell Optimal Design by Computational Fluid Dynamics Testing and Hydrodynamic Analysis. *Energies* **2013**, *6*, 2362–2385. [CrossRef]

59. San, M.; Nyi, N. Design of Cross Flow Turbine and Analysis of Runner's Dimensions on Various Head and Flow Rate. *Int. J. Sci. Res. Publ.* **2018**, *8*, 586–593.
60. Killingtveit, Å. Hydroelectric Power. In *Future Energy*; Elsevier: London, UK, 2020; pp. 315–330.
61. Gernaat, D.; Bogaart, P.; Vuuren, D.; Biemans, H.; Niessink, R. High-resolution assessment of global technical and economic hydropower potential. *Nat. Energy* **2017**, *2*, 821–828. [CrossRef]
62. De Keyser, J.; Fuentes, P.O.; Hayes, D.S.; Habersack, H. A review of hydropower in Central Asia: Past, present, and future. *Renew. Sustain. Energy Rev.* **2026**, *226*, 116239. [CrossRef]
63. Klein, S.; Fox, E. A review of small hydropower performance and cost. *Renew. Sustain. Energy Rev.* **2022**, *169*, 112898. [CrossRef]
64. Amougou, C.; Tsuanyo, D.; Fioriti, D.; Kenfack, J.; Aziz, A.; Elé Abiama, P. LCOE-Based Optimization for the Design of Small Run-of-River Hydropower Plants. *Energies* **2022**, *15*, 7507. [CrossRef]
65. Kaygusuz, K.; Kolay, E. Levelized Cost of Hydropower Projects for Sustainable Electricity Generation. *J. Eng. Res. Appl. Sci.* **2025**, *14*, 86–94.

Disclaimer/Publisher's Note: The statements, opinions and data contained in all publications are solely those of the individual author(s) and contributor(s) and not of MDPI and/or the editor(s). MDPI and/or the editor(s) disclaim responsibility for any injury to people or property resulting from any ideas, methods, instructions or products referred to in the content.